REPORT DOCUMENTATION PAGE

Form Approved
OMB No. 0704-0188

AD-A239 510

2. REPORT DATE	3. REPORT TYPE AND DATES COVERED
June 1991	Final

Mean-Square Error Due to Gradiometer Field Measuring Devices

5. FUNDING NUMBERS

PE 61102F
PR 2313
TA V1
WU 23

6. AUTHOR(S)
Charles P. Hatsell

7. PERFORMING ORGANIZATION NAME(S) AND ADDRESS(ES)
Armstrong Laboratory
Aeronautical Systems Division (AFSC)
Wright-Patterson, AFB, OH 45433

8. PERFORMING ORGANIZATION REPORT NUMBER

AAMRL-TR-89-051

9. SPONSORING/MONITORING AGENCY NAME(S) AND ADDRESS(ES)

Armstrong Laboratory
AL/CF
Brooks AFB, TX 78235-5000

10. SPONSORING/MONITORING AGENCY REPORT NUMBER

11. SUPPLEMENTARY NOTES

Submitted to IEEE Transactions on Biomedical Engineering, Vol. 38, no. 6 (June 1991)

12a. DISTRIBUTION/AVAILABILITY STATEMENT

Approval for public release; distribution is unlimited.

12b. DISTRIBUTION CODE

13. ABSTRACT (Maximum 200 words)

Gradiometers use spatial common mode magnetic field rejection to reduce interference from distant sources. They also introduce distortion that can be severe, rendering experimental data difficult to interpret. Attempts to recover the measured magnetic field from the gradiometer output will be plagued by the nonexistence of a spatial function for deconvolution (except for first-order gradiometers), and by the high-pass nature of the spatial transform that emphasizes high spatial frequency noise. Goals of a design for a facility for measuring biomagnetic fields should be an effective shielded room and a field detector employing a first-order gradiometer.

14. SUBJECT TERMS
Magnetic field measurement
Signal processing
Gradiometers
Magnetic field distortion

15. NUMBER OF PAGES
5

16. PRICE CODE

17. SECURITY CLASSIFICATION OF REPORT	18. SECURITY CLASSIFICATION OF THIS PAGE	19. SECURITY CLASSIFICATION OF ABSTRACT	20. LIMITATION OF ABSTRACT
Unclassified	Unclassified	Unclassified	None

GENERAL INSTRUCTIONS FOR COMPLETING SF 298

The Report Documentation Page (RDP) is used in announcing and cataloging reports. It is important that this information be consistent with the rest of the report, particularly the cover and title page. Instructions for filling in each block of the form follow. It is important to ***stay within the lines*** to meet ***optical scanning requirements***.

Block 1. Agency Use Only *(Leave blank)*.

Block 2. Report Date. Full publication date including day, month, and year, if available (e.g. 1 Jan 88). Must cite at least the year.

Block 3. Type of Report and Dates Covered. State whether report is interim, final, etc. If applicable, enter inclusive report dates (e.g. 10 Jun 87 - 30 Jun 88).

Block 4. Title and Subtitle. A title is taken from the part of the report that provides the most meaningful and complete information. When a report is prepared in more than one volume, repeat the primary title, add volume number, and include subtitle for the specific volume. On classified documents enter the title classification in parentheses.

Block 5. Funding Numbers. To include contract and grant numbers; may include program element number(s), project number(s), task number(s), and work unit number(s). Use the following labels:

C	- Contract	PR	- Project
G	- Grant	TA	- Task
PE	- Program Element	WU	- Work Unit Accession No.

Block 6. Author(s) Name(s) of person(s) responsible for writing the report, performing the research, or credited with the content of the report. If editor or compiler, this should follow the name(s).

Block 7. Performing Organization Name(s) and Address(es) Self-explanatory

Block 8. Performing Organization Report Number. Enter the unique alphanumeric report number(s) assigned by the organization performing the report

Block 9. Sponsoring/Monitoring Agency Name(s) and Address(es) Self-explanatory

Block 10. Sponsoring/Monitoring Agency Report Number *(If known)*

Block 11. Supplementary Notes Enter information not included elsewhere such as: Prepared in cooperation with ; Trans. of ; To be published in . When a report is revised, include a statement whether the new report supersedes or supplements the older report.

Block 12a. Distribution/Availability Statement. Denotes public availability or limitations. Cite any availability to the public. Enter additional limitations or special markings in all capitals (e.g. NOFORN, REL, ITAR).

- **DOD** - See DoDD 5230.24, "Distribution Statements on Technical Documents."
- **DOE** - See authorities.
- **NASA** - See Handbook NHB 2200.2.
- **NTIS** - Leave blank.

Block 12b. Distribution Code.

- **DOD** - Leave blank.
- **DOE** - Enter DOE distribution categories from the Standard Distribution for Unclassified Scientific and Technical Reports.
- **NASA** - Leave blank.
- **NTIS** - Leave blank.

Block 13. Abstract. Include a brief *(Maximum 200 words)* factual summary of the most significant information contained in the report.

Block 14. Subject Terms. Keywords or phrases identifying major subjects in the report.

Block 15. Number of Page Enter the total number of pages.

Block 16. Price Code. Enter appropriate price code *(NTIS only)*.

Blocks 17. - 19. Security Classifications. Self-explanatory. Enter U.S. Security Classification in accordance with U.S. Security Regulations (i.e., UNCLASSIFIED) If form contains classified information, stamp classification on the top and bottom of the page.

Block 20. Limitation of Abstract This block must be completed to assign a limitation to the abstract. Enter either UL (unlimited) or SAR (same as report). An entry in this block is necessary if the abstract is to be limited If blank, the abstract is assumed to be unlimited.

Mean-Square Error Due to Gradiometer Field Measuring Devices

Charles P. Hatsell

Abstract—**Gradiometers use spatial common mode magnetic field rejection to reduce interference from distant sources. They also introduce distortion that can be severe, rendering experimental data difficult to interpret. Attempts to recover the measured magnetic field from the gradiometer output will be plagued by the nonexistence of a spatial function for deconvolution (except for first-order gradiometers), and by the high-pass nature of the spatial transform that emphasizes high spatial frequency noise. Goals of a design for a facility for measuring biomagnetic fields should be an effective shielded room and a field detector employing a first-order gradiometer.**

I. Introduction

MEASUREMENT distortions introduced by commonly used biomagnetic field measuring devices are addressed in this paper. Comment is also made on the difficulties encountered attempting to infer the actual magnetic field from the distorted estimate provided by the instrument. Effects of instrument noise are also discussed. Measurement of extracorporeal magnetic fields arising from intracorporeal ionic fluxes (viz., biomagnetic fields) requires solving two fundamental problems: achieving high gain, low noise amplification and reducing the effect of interfering environmental magnetic fields (e.g., the earth's magnetic field, fields associated with fixed wiring). The former problem is traditionally solved by employing as an amplifier a superconducting quantum interference device (SQUID) [1].

Rejection of local, interfering fields (which may be 6 to 10 orders of magnitude larger than the biological fields of interest) is in part and almost universally approached by using a detector coil configured to reject low-order field gradients. The rationale for spatial common-mode rejection is that the far field of a source tends to contain predominantly low-order spatial components. The most popular coil configuration is a second-order gradiometer with coaxial, equal-area coils as shown in Fig. 1. Practically, a second order gradiometer has become widely accepted as a reasonable tradeoff between interference rejection and instrument sensitivity. There is an extensive literature discussing various gradiometer configurations that will not be repeated here [2]; especially relevant is a discrete spatial filtering approach to gradiometer design investigated by Bruno *et al.* [6].

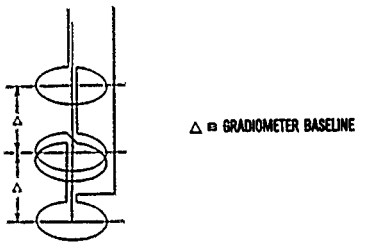

Fig. 1. Second-order gradiometer. Coils are of equal area and coaxial, with the center coil wound in opposite sense to the outer coils. Δ, distance between adjacent coils is the gradiometer baseline.

A critical gradiometer dimension is its baseline, Δ. Small Δ enhances common-mode rejection but decreases sensitivity and increases spatial distortion in the measured or apparent field (i.e., the apparent field differs from that field that would have been measured with a zero-order gradiometer, also called a magnetometer). Large Δ reduces distortion and increases sensitivity but at the cost of decreased common-mode rejection.

In any case, the apparent field as measured by the gradiometer is not the actual field at all, but some mildly to severely distorted version. It is this distortion and its mitigation that are addressed here. The error that finite coil area introduces over a point measurement has been addressed elsewhere [3]; so to focus attention on the subject at hand, it will be ignored here.

II. The Apparent Field

Suppose our second-order gradiometer is aligned along the z-axis as in Fig. 2. If the field strength at the lower gradiometer coil at $z = 0$ is $H_z(x, y, z)$, then the apparent field measured by the second-order gradiometer would be

$$G_z^2(x, y, z) = H_z(x, y, z) - 2H_z(x, y, z + \Delta) + H_z(x, y, z + 2\Delta) \quad (1)$$

and it follows directly that for equal coil cross-section, an nth-order gradiometer would give

$$G_z^n = \sum_{m=0}^{n} \binom{n}{m} (-1)^m H_z(x, y, z + m\Delta). \quad (2)$$

Manuscript received August 8, 1990; revised July 13, 1990.

The author was with the Harry G. Armstrong Aerospace Medical Research Laboratory, Wright-Patterson Air Force Base, OH. He now with the Human Systems Division, HSD/XA, Brooks Air Force Base, TX 78235.

IEEE Log Number 9144685.

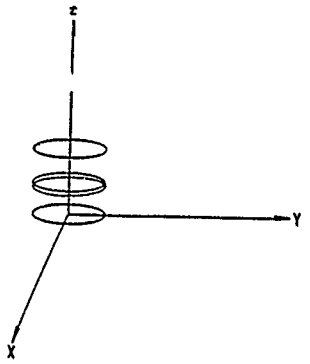

Fig. 2. Second-order gradiometer aligned with z-axis.

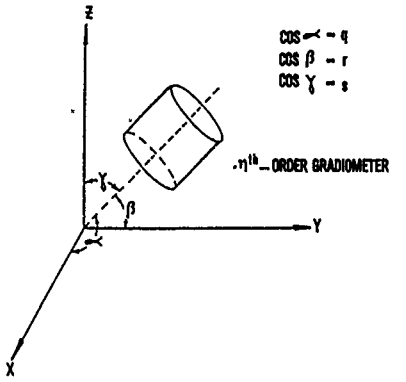

Fig. 3. nth-order gradiometer aligned with an axis with direction cosines q, r, and s.

While the second-order gradiometer is clearly most popular, the following development will be for nth-order equal coil area gradiometers.

Consider an nth-order gradiometer oriented as shown in Fig. 3. The center of the lower coil is located at (x, y, z), and the direction cosines of the gradiometer axis are q, r, s giving

$$q^2 + r^2 + s^2 = 1 \tag{3}$$

and

$$\vec{u} = q\vec{a}_x + r\vec{a}_y + s\vec{a}_z \tag{4}$$

where $\vec{u}$ is the unit vector of the gradiometer axis and $\vec{a}_x$, $\vec{a}_y$, $\vec{a}_z$ are the coordinate axis unit vectors. In a manner similar to that leading to (2), the apparent field measured by an nth-order, equal coil area gradiometer is

$$\vec{G}^n(x, y, z) = \sum_{m=0}^{n} \binom{n}{m} (-1)^m \vec{H}(x + mq\Delta, y + mr\Delta, z + ms\Delta). \tag{5}$$

III. Mean-Square Measurement Error

Throughout, a source-free measurement space is assumed so the magnetic field $\vec{H}$ is conservative and determined by its scalar potential, φ;

$$\vec{H} = -\nabla\varphi \tag{6}$$

and

$$\nabla^2\varphi = 0. \tag{7}$$

A vector measurement error is defined to be $\vec{K}$, where

$$\vec{K} = \vec{H} - \vec{G} \tag{8}$$

and the following scalar potentials are implicitly defined:

$$\vec{G} = -\nabla\varphi_g \tag{9}$$

and

$$\vec{K} = -\nabla\psi \tag{10}$$

where φ_g is the scalar potential associated with the apparent field $\vec{G}$. If a volume V of this source-free space is enclosed by a surface S, then from Green's first identity and the fact that $\nabla^2\psi = 0$ (measurement uncertainties are ignored),

$$\int_V \nabla\psi \cdot \nabla\psi \, d\tau = \int_S \psi\nabla\psi \cdot d\vec{S}. \tag{11}$$

Now let $\vec{n}$ be the unit normal to the surface S, and define a differential volume dV enclosed by S and an external surface S' everywhere ϵ distant from S. Again from Green's theorem

$$\int_{dV} \nabla\psi \cdot \nabla\psi \, d\tau = \int_{S'} \psi\nabla\psi \cdot d\vec{S}' - \int_S \psi\nabla\psi \cdot d\vec{S}. \tag{12}$$

With $d\vec{S} = \vec{n}\, ds$, and $d\vec{S}' = \vec{n}'\, ds$, an approximation for (12) is

$$\epsilon \int_S \nabla\psi \cdot \nabla\psi \, ds \approx \int_{S'} \psi\nabla\psi \cdot \vec{n}' \, ds - \int_S \psi\nabla\psi \cdot \vec{n} \, ds \tag{13}$$

which as $\epsilon \to 0$ gives

$$\int_S \nabla\psi \cdot \nabla\psi \, ds = \frac{\partial}{\partial\vec{n}} \int_S \psi\nabla\psi \cdot d\vec{S}. \tag{14}$$

Note that the left-hand side of (14) is the integrated-square field measurement error caused by measuring with a gradiometer rather than a magnetometer.

IV. An Example

The familiar case of a current dipole embedded a units beneath a semi-infinite volume conductor will be addressed. The dipole is taken as y-directed and the surface normal is $\vec{n} = \vec{a}_z$. For this conductor geometry (14) becomes

$$\int_{-\infty}^{\infty}\int_{-\infty}^{\infty} \nabla\psi \cdot \nabla\psi \, dx \, dy = \frac{\partial^2}{\partial z^2} \int_{-\infty}^{\infty}\int_{-\infty}^{\infty} \frac{\psi^2}{2} \, dx \, dy. \tag{15}$$

It may be verified directly [4] that for this geometry the solution to Laplace's equation is

$$\psi = \iint E(\alpha, \beta) \exp(i2\pi\alpha x + i2\pi\beta y) \cdot \exp[-2\pi(\alpha^2 + \beta^2)^{1/2} z]\, d\alpha\, d\beta \quad (16)$$

where $E(\alpha, \beta)$ is the two-dimensional Fourier transform of ψ over the xy plane for fixed z and is determined from boundary conditions; α and β are variables of integration. Applying Parseval's theorem to (15), the square measurement error M becomes

$$M = \iint (\alpha^2 + \beta^2)|E(\alpha, \beta)|^2\, d\alpha\, d\beta \quad (17)$$

where

$$|E|^2 = |F|^2\,|1 - T|^2 \quad (18)$$

and, from Cuffin and Cohen [5],

$$F(\alpha, \beta) = iP_y\alpha \exp[-2\pi a(\alpha^2 + \beta^2)^{1/2}/[4\pi(\alpha^2 + \beta^2)] \quad (19)$$

on the $z = 0$ plane; P_y is the current dipole moment. Note that (2) expresses the gradiometer output as a linear combination of H_z shifted in z; therefore, in the transform domain there will be some function $T(\alpha, \beta)$ that relates the transform of G_z^n, say g_z^n to the transform of H_z, say h_z in the following manner

$$g_z^n(\alpha, \beta) = T(\alpha, \beta) \cdot h_z(\alpha, \beta). \quad (20)$$

Hence (2) may be expressed in the transform domain as

$$g_z^n(\alpha, \beta) = h_z(\alpha, \beta) \cdot \sum_{m=0}^{n} \binom{n}{m} (-1)^m \cdot \exp[-2\pi m(\alpha^2 + \beta^2)^{1/2}\Delta] \quad (21)$$

and it follows from the binomial theorem that

$$T(\alpha, \beta) = [1 - \exp(-2\pi(\alpha^2 + \beta^2)^{1/2}\Delta)]^n. \quad (22)$$

It is useful to accomplish (17) in polar coordinates by the substitutions $\alpha = \rho\cos\theta$, $\beta = \rho\sin\theta$, and $d\alpha\, d\beta = \rho\, d\rho\, d\theta$, resulting in

$$M = [P_y/(4\pi)^2] \int_0^{\infty} \int_0^{2\pi} \cdot \cos^2\theta e^{-4\pi a\rho}|1 - T|^2\, \rho\, d\rho\, d\theta. \quad (23)$$

This integral can be evaluated in closed form. The result when expressed as a fraction e of the total magnetic field energy is

$$e = 1 - 8(a/\Delta)^2 \sum_{m=0}^{n} \binom{n}{m} (-1)^m/(2a/\Delta + m)^2 + 4(a/\Delta)^2 \sum_{m=0}^{2n} \binom{2n}{m} (-1)^m/(2a/\Delta + m)^2 \quad (24)$$

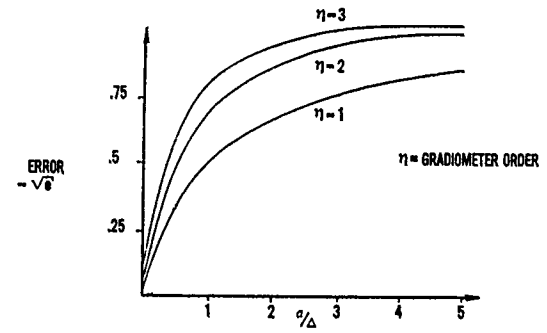

Fig. 4. Root-integrated-square-measurement error due to a gradiometer of order n and baseline Δ. Current source is a dipole parallel to and a units beneath the planar surface of a conducting half-space. e is given by (24).

which is seen to be dependent only on the ratio of dipole depth a to gradiometer baseline Δ and gradiometer order n. Fig. 4 shows a plot of this result for several representative parameters.

V. Magnetic Field Recovery

The previous development suggests an inverse transform technique may be useful for recovery of the magnetic field spatial distribution from the gradiometer output spatial distribution. This technique would involve computing the *spatial* Fourier transform of the gradiometer output data and then inverting the product of this transform with $1/T(\alpha, \beta)$ and an appropriate window function. Equivalently, deconvolution could be performed in the spatial domain by convolving the gradiometer data with the inverse transform of $1/T(\alpha, \beta)$, applying an appropriate spatial window. Unfortunately, several problems would arise in such an attempt.

Spatial deconvolution without windowing is not possible because $1/T(\alpha, \beta)$ is not Fourier invertable, and even with low-pass windowing is noninvertable for gradiometer order greater than one due to the singularity at the origin in transform space. Invertability would require a window that is zero in the vicinity of the transform space origin; this could produce acceptable results were it not for noise contributed by the instrument proximal to the gradiometer. This *temporal* noise process, which is assumed zero-mean with rms value n_0, produces a *spatial* white noise process of zero-mean with mean-square value η_0 given by

$$\eta_0 = (n_0)^2\pi \int |W(\rho)/T(\rho)|^2\, \rho\, d\rho \quad (25)$$

where $\rho = \sqrt{\alpha^2 + \beta^2}$, and $W(\rho)$ is a windowing function with properties as previously discussed.

As an example, the dipole model previously discussed will be used. Let $W(\rho)$ be a Hanning window modified as follows:

$$W(\rho) = \begin{cases} 0, & \rho \le \rho_\epsilon, \\ \left[1 + \cos\left(\dfrac{\rho}{\rho_m}\pi\right)\right]\Big/2, & \rho_\epsilon < \rho \le \rho_m, \\ 0, & \rho > \rho_m, \end{cases} \quad (26)$$

where ρ_m is chosen to encompass a fraction $\mathcal{F}$ of the energy in the current dipole, and $\rho_\epsilon = \rho_m/100$. Using (19), it is easy to show that

$$\rho_m = \frac{1}{4\pi a}\left[\ln\frac{1+4\pi a}{1-\mathcal{F}}\right] \tag{27}$$

where the energy excluded for $\rho_\epsilon > 0$ has been ignored.

Since the additive noise is zero-mean, the expected value of the conditional mean estimate is the inverse of its windowed spatial transform, i.e.,

$$E\{\hat{H}_z(x, y)\} = \int\int h_z(\alpha, \beta)\, W(\rho) \cdot \exp(i2\pi\alpha x + i2\pi\beta y)\, d\alpha\, d\beta \tag{28}$$

where $\rho = \sqrt{\alpha^2 + \beta^2}$, h_z is the two dimensional transform of H_z, $\hat{H}_z$ is the estimate of H_z, and $E\{\cdot\}$ denotes expectation.

$E\{\hat{H}_z(x, y)\}$ can be calculated for the dipole model by using (19) and (26) in (28) and transforming to polar coordinates as was done in (23). Integrating first over θ gives for the $z = 0$ plane

$$E\{\hat{H}_z(x, y)\}|_{z=0} = \frac{\pi P_y x}{\sqrt{x^2 + y^2}} \int_{\rho_\epsilon}^{\rho_m} W(\rho) \cdot e^{-2\pi a\rho} J_1(2\pi\rho\sqrt{x^2 + y^2})\rho\, d\rho \tag{29}$$

where $J_1(\cdot)$ is the Bessel function of the first kind of order one. This integral was evaluated numerically in the examples to follow; it converges rapidly.

Typical instruments used for magnetic field measurements have a noise floor of about 20 femtotesla $(fT)/\sqrt{Hz}$, so an instrument temporal bandwidth of 100 Hz would produce an rms noise output of about 0.2 picotesla (pT). Usually, in an evoked response paradigm some averaging is done that for k averages would reduce the rms noise by $1/\sqrt{k}$. Maximum evoked fields from the brain can be expected to be about 0.5 pT.

Fig. 5 shows the z components of the true field, gradiometer output, and expected field estimate as given by (29), using the modified Hanning window for a second-order gradiometer of baseline 2 cm, dipole depth of 1 cm, and 10 averages. Fig. 6 is similar but assumes a dipole depth of 2 cm. In each case the temporal rms noise is 0.2 pT, $\mathcal{F} = 0.95$, and the dipole moment has been adjusted to produce a true field peak of 0.5 pT. Note that even though the estimate mean appears good, especially for the deeper source, the rms error is quite large, even for 10 averages. Certainly for single event analysis of brain evoked fields, instrument noise would be prohibitively large, however, larger biomagnetic fields such as those from the myocardium might be recovered effectively using these techniques.

As mentioned in the Introduction, any practical application of this technique would require accounting for gradiometer coil area, because additional singularities are introduced into $1/T(\alpha, \beta)$ placing further constraints on selection of ρ_m. Finally, the reader is referred to a recent paper by Bruno *et al.* [7] in which an interesting but somewhat different approach to spatial filtering of gradiometer output is discussed. Their approach will also have significant problems with instrument noise; however, they deferred an analysis of the effect.

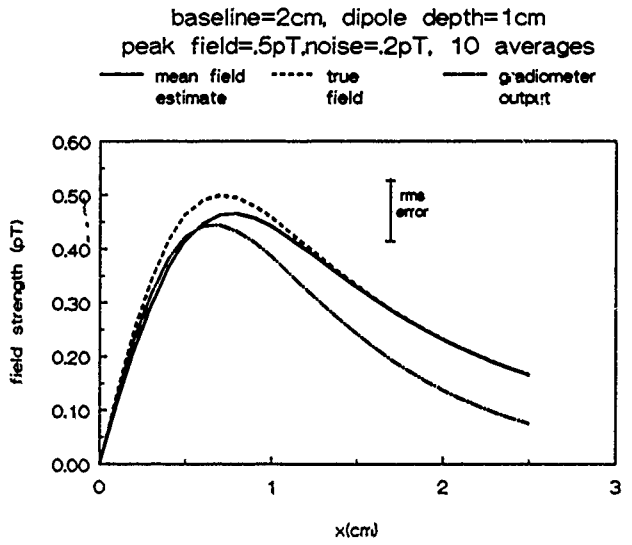

Fig. 5. True magnetic field z-component, its estimate using transform techniques, and the output of the gradiometer from which the estimate was derived. Measurement is along the x-axis at $z = 0$. Current source is a y-directed dipole parallel to and 1 cm beneath the planar ($z = 0$) surface of a conducting half-space. Dipole moment is such that the magnetic field peak is 0.5 pT.

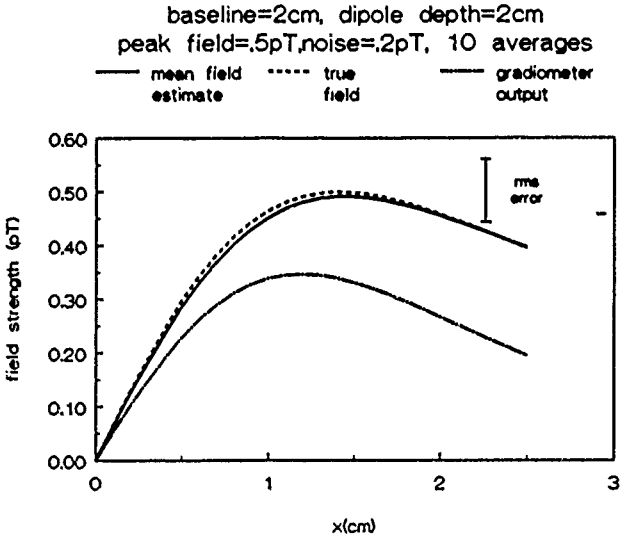

Fig. 6. As in Fig. 5, but the dipole depth is 2 cm.

VI. Discussion

It is clear that unless the gradiometer baseline is at least several times the source depth significant error will result from any attempt at detailed analysis of the magnetic fields arising from current sources of interest. Although many investigators have without doubt been impressed with the effectiveness of spatial common mode rejection, the data

collected have been in many cases severely distorted. Attempts to correct these errors through decorrelation using the inverse transform of $1/T(\alpha, \beta)$ will not be possible because its inverse does not exist, and because it is a high-pass function its use in an inverse transform technique will emphasize high spatial frequency noise components.

It should be noted that the explicit inversion technique explored in this paper is model independent i.e., if constraints on the magnetic field structure are available, a model may be useful in realizing additional improvements in signal-to-noise ratio. For example, some evoked response paradigms used in magnetoencephalography will produce relatively concentrated neural activity in the brain [2]. Such concentrated activity might be modeled as a dipole source and the data used in a parameter estimate determining a best fit (e.g., least-square) to the dipole model. Such "additional" *a priori* information may lead to significant noise reduction, and in that sense an explicit inversion technique that ignores this information incurs a relative penalty. Also, instruments with multiple, spatially distributed gradiometers can realize noise reduction through spatial processing techniques. In any case, the inversion techniques discussed here can be applied at an appropriate place in the analysis to reduce the distortion introduced by the gradiometer.

The analysis contained herein strongly suggests that any laboratory investigating biomagnetic fields consider a room that rejects interfering fields and an instrument employing a low order gradiometer. Certainly, a first order device should be a goal.

Acknowledgment

The particularly thorough and constructive reviews given this paper by the referees were very helpful to the author.

References

[1] J. Clarke, "Superconducting quantum interference devices for low frequency measurements," *Superconductor Applications: SQUID's and Machines*, B. B. Schwartz and S. Foner, Eds. New York: Plenum Press, 1977.

[2] S. J. Williamson *et al.*, *Biomagnetism: An Interdisciplinary Approach*. New York: Plenum Press, 1982.

[3] B. J. Roth *et al.*, "Using a magnetometer to image a two-dimensional current distribution," *J. Appl. Phys.*, vol. 65, no. 1, pp. 361-372.

[4] N. Tralli, *Classical Electromagnetic Theory*. New York: McGraw-Hill, 1963.

[5] N. Cuffin and D. Cohen, "Magnetic fields of a dipole in special volume conductor shapes," *IEEE Trans. Biomed. Eng.*, vol. BME-24, pp. 372-381, 1977.

[6] A. C. Bruno *et al.*, "Discrete spatial filtering with SQUID gradiometers in biomagnetism," *J. Appl. Phys.*, vol. 59, no. 7, pp. 2584-2589, Apr. 1986.

[7] ——, "Planar gradiometer input signal recovery using a Fourier technique," in *Biomagnetism '87, Proc. 6th Int. Conf. Biomagnetism*, K. Atsumi *et al.*, Eds. Tokyo: Tokyo Denki Univ. Press, 1988, pp. 454-457.

Charles P. Hatsell was born in Alexandria, VA in 1944. He received the B.S. degree from Virginia Polytechnic Institute, Blacksburg, VA, the M.S. and Ph.D. degrees from Duke University, Durham, NC, and the M.D. degree from the University of Miami, Coral Gables, FL.

In 1971 he entered active duty with the U.S. Air Force where he has held several clinical and research positions. Currently, he is Deputy Program Director for Science, Technology, and Operational Aeromedical Support, Human Systems Division, Air Force Systems Command. His research interests include neurophysiology and biomagnetic field measurement.

Dr. Hatsell is a member of the Aerospace Medical Association, American Medical Association, American College of Preventive Medicine, Phi Kappa Phi, Eta Kappa Nu, Tau Beta Pi, and Sigma Xi.